Influence of Surface Oxygen Vacancies on the Photocatalytic Activity of Nanocrystalline TiO_2

Hua-rong Zhang [a)]**, Hai-wu Zheng, Yu-zong Gu, Yong Liang, Yu-rui Cao, Ke-qi Tan**
Institute of Microsystemic Physics and School of Physics & Electronics, Henan University, Kaifeng 475001, People's Republic of China
School of Physics & Electronics, Henan University, Kaifeng 475001, People's Republic of China
Email:zhanghr@henu.edu.cn

Abstract: The influence of surface oxygen vacancies on the photo-generated charge carrier separation and photocatalytic activity in nanocrystalline TiO_2 has been investigated in this work. The X-ray photoelectron spectra reveal that more surface oxygen vacancies are produced in the air-annealing sample compared to the oxygen-annealing sample. It is found that more oxygen vacancies produce more recombination centers, which causes weaker intensity of the surface photovoltaic spectroscopy signal in the air-annealing sample due to lower separation rate of photo-generated charge carriers. Simultaneously, more oxygen vacancies also yield more photocatalytic reactive centers and improve the photocatalytic activity for the air-annealing sample.

Keywords: TiO_2; Oxygen vacancy; Photogenerated charge carrier; Photocatalytic activity

1. Introduction

Nanocrystalline TiO_2 has been extensively investigated and proven to be one of the most promising photocatalysts widely used in wastewater treatment and hydrogen generation [1]. However, low sunlight absorption efficiency and high recombination rate of photo-generated charge carriers prevent the widely applications of TiO_2 in the environmental realm. To enhance response to visible-light and reduce recombination of photo-generated electrons and holes, a great deal of effort has been devoted by doping with various metal cations, nonmetal anions or codoping with two different elements [2-9]. Among these works, N doped TiO_2 was frequently reported and was found to exhibit greatly enhanced visible-light response and photocatalytic activity [5-9]. Ihara *et al.* stated that the oxygen vacancies induced by N doping played an important role in the visible-light activity and photocatalytic property [9]. However, it is difficult to confirm the effects of oxygen vacancies on the optical absorption and photocatalytic activity in the N doped TiO_2 because other factors such as N impurity level can also cause the variations of these properties [6]. Therefore, some experimental works to investigate the direct relation between photocatalytic performance and oxygen vacancies in TiO_2 catalyst are important and interesting. Practically there are a number of investigations on the oxygen vacancies in TiO_2 [9-14]. For example, Nakamura *et al.* [11] demonstrated that the appearance of the visible light activity in the plasma-treated TiO_2 photocatalyst was ascribed to the newly formed oxygen vacancy state between the valence and the conduction bands in the TiO_2 band structure. The theoretical and experimental results by Justicia *et al.* [10] also suggested that the gap-narrowing induced by the presence of oxygen vacancies was responsible for the enhanced optical activity in the visible range.

In our previous work [14], the different surface oxygen defect states had been reported to result in the different spectroscopic properties in nanocrystalline TiO_2 thermally treated under different atmospheres. In this work, the further measurements, involving the characterizations of X-ray photoelectron spectroscopy (XPS), surface photovoltaic spectroscopy (SPS) and photocatalytic activity, have been systemically carried out . It is found that the surface oxygen vacancies in nanocrystalline TiO_2 play an important role in the processes of photocatalytic degradation by comparing the differences of photocatalytic performance between the samples annealing under air and oxygen atmosphere.

2. Experimental

The anatase nanocrystalline TiO_2 was synthesized by a simple sol-gel method. The mixture solution of 10 mL of

978-1-935068-41-9 © 2010 SciRes.

titanium(Ⅳ) *n*-butoxide ($Ti(OBu)_4$) and 40 of mL anhydrous ethanol was added dropwise into another mixture solution consisting of 10 mL of deionized water, 10 mL of ethanol and 2 mL of 70% nitric acide at room temperature under roughly stirring. The light yellowish transparent sol was obtained after continuously stirring for 3 hours. After standing at room temperature for 6 hours, the sol was dried at 70 ˚C for 36 hours. The TiO_2 gel was formed, which was put into a tube furnace and calcined at 500 ˚C for 6 hours under air and flowing oxygen, respectively. The furnace was cooled to room temperature, then the anatase nanocrystalline TiO_2 was yielded. XPS measurements were recorded on an Axis Ultra system with monochromatic Al Kα X rays (1486.6ev) operated at 45 W and 15 kV with a background pressure of approximately 5.0×10^{-9} Torr. A survey spot size and 40 eV pass energy were used for the analysis. Emitted photoelectrons perpendicular to the sample surface were collected. The binding energy of all investigated elements were referenced by the C *1s* peak at 284.8 eV of the surface adventitious carbon, respectively. The SPS measurements were carried out with a home-built apparatus which consisted of a 500 W xenon lamp (CHF XQ500W, China), a double-grating monochromator (Zolix SP500), a lock-in amplifier (SR830-DSP), and a light chopper (SR540). Photocatalytic experiments were carried out in an inner-irradiation-type reactor. A cylindric reaction cell was used to contain the reaction solution and a 500 W long-arc xenon lamp surrounded with a water cooling system was fixed in the center of the reaction cell. 0.2 g of photocatalyst was suspended in 200 mL of a methylene blue (MB) solution (10 mg/L) under stirring magnetically. The mixture was kept in the dark for 30 minutes to establish an adsorption-desorption equilibrium before the light radiation. The amount of MB in the solution was determined on the basis of its characteristic optical absorption at 665 nm using a 723 spectrophotometer.

3. Results and discussion

The structural characterizations about X-ray diffraction and Raman spectra of the samples were described in our previous published work [14]. Typical XPS spectra of Ti *2p* core level for the samples of air-annealing and oxygen-annealing are, respectively, exhibited in Fig. 1. Two XPS peaks of the Ti $2p_{3/2}$ and Ti $2p_{1/2}$ can be found in the figure. The inset of Fig. 1 presents the enlarged curve of Ti $2p_{3/2}$ peak. It can be seen that the Ti $2p_{3/2}$ peak of the sample annealing under air slightly shift towards lower binding energy as compared to that of the oxygen-annealing sample. By fitting the peaks, it is obtained that Ti $2p_{3/2}$ peak are located at 456.77 eV and 456.82 eV for the samples annealing under air and oxygen atmosphere, respectively. Similar results have been reported by several other groups [12, 15-17], where the peak position shift to lower binding energy is attributed to the formation of oxygen vacancies in TiO_2 [17]. As our previous work discussed [14], the thermal treatment at high temperature will cause the surface lattice oxygen diffusion into external environment [18], resulting in the formation of more amount of dangling bonds or oxygen vacancies on the surface of TiO_2. Offering the heat treatment with oxygen atmosphere can hold back the escape of surface oxygen due to higher surrounding oxygen pressure. Thus, more surface oxygen vacancies exist on the nanoparticles surface of the air-annealing sample than that of the sample annealing under oxygen atmosphere, which conduce the XPS peak position shift towards lower binding energy as compared to the oxygen-annealing sample. Herein, the difference of surface oxygen vacancies concentration in two samples is further confirmed by the XPS results of the samples.

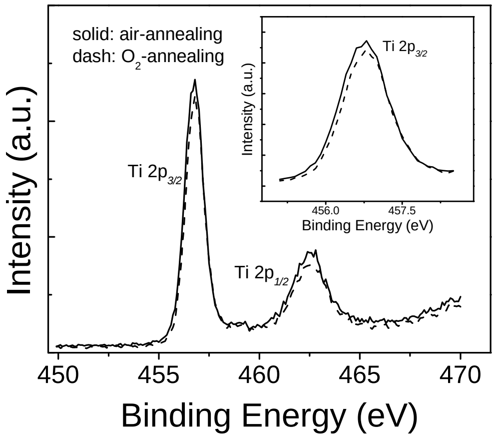

Fig. 1. XPS spectra of Ti *2p* core level for the samples annealing under air (solid line) and oxygen atmosphere (dash line). The inset presents the enlarged curve of Ti $2p_{3/2}$ peak.

Fig. 2 shows the SPS responses of the TiO_2 samples. It is found that two samples exhibit obvious surface photovoltaic response with wavelength range from 320 nm to 420 nm. It must be noted that greatly enhanced signal intensity is observed in the SPS of the sample annealing under oxygen atmosphere compared to the sample annealing under air. It is well known that SPS measurement can provide information about surface charge distribution and band gap in semiconductors. Generally, the higher the surface photovoltaic signal, the higher the separation rate of photo-induced charge carriers [19]. As is discussed above, more surface oxygen vacancies exist on the surface of nanoparticles of the air-annealing sample than that of the oxygen-annealing sample. These oxygen vacancies can act as charge carrier recombination centers and promote the recombination process of photo-induced electrons and holes [20], resulting in the lower separation rate of photo-induced charge carriers in the sample annealing under air. Consequently, greatly enhanced signal intensity in the SPS of the oxygen-annealing sample can be attributed to less oxygen vacancies on the surface of the sample than that of the sample annealing under air, which is consistent with the results of photoluminescence (PL) spectra of the samples in our previous work [14]. As the literature reported, the intensity of the PL band was enormously weakened in the sample annealing in oxygen compared to the sample annealing in air because of more oxygen defects concentration in the latter. The PL emission is the result of the recombination of excited electrons and holes, the lower PL intensity of the sample indicates a lower recombination rate [8, 21]. On the other hand, as shown in Fig. 2, the SPS peak of the sample annealing under oxygen atmosphere is centered at a longer wavelength than that of the sample annealing under air, which agrees with the red-shift in the absorption spectra of the samples [14]. As our previous stated, the red-shift in the absorption spectra can be interpreted by Burstein-Moss effect. Based on Burstein-Moss effect, the increase of oxygen deficiency will broaden the optical band gap and lead the blue shift of absorption spectra for oxide semiconductors. It is well known that the mechanism of photo response in SPS is same as that in absorption spectrum. Accordingly, compared to the air-annealing sample, the red-shift in the SPS results can also attributed to the optical band gap narrowing due to the decrease of oxygen vacancies in the oxygen-annealing sample.

The photocatalytic activity of the samples annealing under air and oxygen atmosphere are, respectively, evaluated by monitoring the degradation of MB. The curves of *C/C_0 vs irradiation time* (C and C_0 are the remanent and original concentration of MB, respectively) are shown in **Fig. 3**. It is found that the sample annealing under air presents better photocatalytic degradation rate of MB than the oxygen-annealing sample, which is contradict with the absorption spectra and SPS results of the samples because both the red-shift in the absorption spectra and increasing signal intensity in the SPS for the oxygen-annealing sample are in favor of the photocatalytic activity of TiO_2. According to above discussion, more surface oxygen vacancies exist on the surface of nanoparticles of the air-annealing sample than that of the oxygen-annealing sample. It has been stated that the surface oxygen-deficient site in the sample can interact strongly with exoteric oxygen molecules to form O_2^- [22]. O_2^- is an efficient electron scavenger [23] which can trap a photo-induced electron and then form two O^-. The formation of O^- is considered to be very important for photocatalytic oxidation processes [24]. Herein, more surface oxygen vacancies give rise to the formation of more photocatalytic reactive centers of O^-, resulting in the improvement of photocatalytic activity in the sample annealing under air. Therefore, it is indicated that the photocatalytic reactive center induced by oxygen vacancy plays an important role in the photocatalytic activity of TiO_2 catalyst.

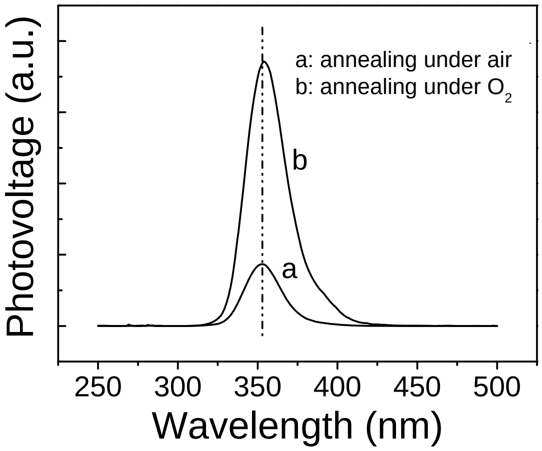

Fig. 2. SPS responses of the nanocrystalline TiO_2 annealing under (a) air and (b) oxygen atmosphere.

4. Conclusions

In conclusion, more oxygen vacancies exist on the surface of the nanocrystalline TiO_2 sample annealing under air compared to the oxygen-annealing sample, which induces the Ti $2p_{3/2}$ peak shift towards lower binding energy in the XPS spectra of the samples. More recombination centers is produced due to the presence of more oxygen vacancies, which causes the lower separation rate of photoinduced charge carriers in the air-annealing sample, resulting in the decrease of the SPS signal intensity. However, the oxygen-annealing sample does not present better photocatalytic activity although it exhibits better optical obsorption performance and higher separation rate of photoinduced charge carriers compared to the sample annealing under oxygen atmosphere. It can be understood by the formation of more photocatalytic reactive centers induced by oxygen vacancies in the air-annealing sample. It is suggested that the photocatalytic reactive center induced by oxygen vacancy play an important role in the photocatalytic activity of TiO_2 catalyst.

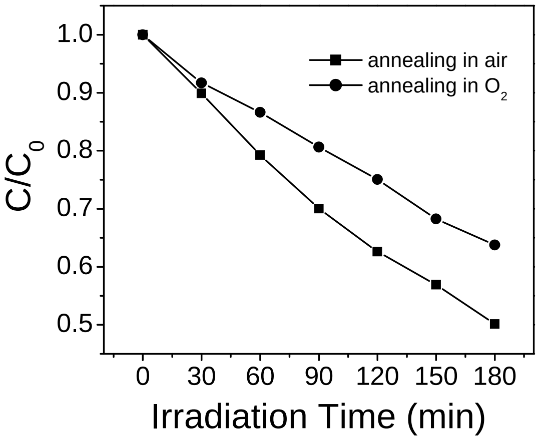

Fig. 3. Photocatalytic degradation ratio of MB in the presence of (a) air-annealing and (b) oxygen-annealing nanocrystalline TiO2.

5. Acknowledgment

This work is financially supported by the Project of Henan Provincial Department of Science and Technology (Grant no. 082300460070).

References（参考文献）

[1] A. L. Linsebigler, G. Lu, and J. T. Yates, Chem. Rev. 95, 735-758, 1995.

[2] J. Soria, J. C. Conesa, V. Augugliaro, M. Schiarello, A. Sclafani, J. Phys. Chem. 95, 274-282,1991.

[3] W. Choi, A. Termin, M. R. Hoffmann, J. Phys. Chem. 98, 13669-13679, 1994.

[4] J. Moon, H. Takagi, Y. Fujishiro, M. Awano, J. Mater. Sci. 36, 949-955, 2001.

[5] K. Q. Tan, H. R. Zhang, C. F. Xie, H. W. Zheng, Y. Z. Gu, W. F. Zhang, doi:10.1016/j.catcom.2009.10.025.

[6] R. Asahi, T. Morikawa, T. Ohwaki, K. Aoki, Y. Taga, Science 293, 269-271, 2001.

[7] T. Ihara, M. Ando, S. Sugihara, Photocatalysis 5, 19, 2001.

[8] Y. Cong, J. Zhang, F. Chen, M. Anpo, D. He, J. Phys. Chem. C 111, 10618-10623, 2007.

[9] T. Ihara, M. Miyoshi, Y. Iriyama, O. Matsumoto, S. Sugihara, Appl. Catal. B 42, 403-409, 2003.

[10] I. Justicia, P. Ordejon, G. Canto, J. L. Mozos, J. Fraxedas, G. A. Battiston, R. Gerbasi, A. Figueras, Adv. Mater. 14, 1399-1402, 2002.

[11] I. Nakamura, N. Negishi, S. Kutsuna, T. Ihara, S. Sugihara, K. J. Takeuchi, J. Mol. Catal. A: Chem. 161, 205-212, 2000.

[12] R. Sanjinés, H. Tang, H. Berger, F. Gozzo, G. Margaritondo, F. Lé vy, J. Appl. Phys. 75, 2945-2951, 1994.

[13] K. Iijima, M. Goto, S. Enomoto, H. Kunugita, K. Ema, M. Tsukamoto, N. Ichikawa, H. Sakama, J. Lumin. 128, 911-913, 2008.

[14] H. R. Zhang, C. F. Xie, Y. F. Zhang, G. S. Liu, Z. H. Li, C. Y. Liu, X. P. Ma, W. F. Zhang, J. Appl. Phys. 103, 103107, 2008.

[15] Z. Q. Jiang, W. H. Zhang, L. Jin, X. Yang, F. Q. Xu, J. F. Zhu, W. X. Huang, J. Phys. Chem. C 111, 12434-12439, 2007.

[16] A. K. Rumaiz, B. Ali, A. Ceylan, M. Boggs, T. Beebe, S. I. Shah, Solid State Commun. 144, 334-338, 2007.

[17] C. M. Huang, X. Q. Liu, Y. P. Liu, Y. Y. Wang, Chem. Phys. Lett. 432, 468-472, 2006.

[18] U. Diebold, Surf. Sci. Rep. 48, 53-229, 2003.

[19] L. Q. Jing, H. G. Fu, B. Q. Wang, D. J. Wang, B. F. Xin, S. D. Li, J. Z. Sun, Appl. Catal. B 62, 282-291, 2006.

[20] H. Irie, Y. Watanabe, K. Hashimoto, J. Phys. Chem. B 107, 5483-5486, 2003.

[21] H. Tang, K. Prasad, R. Sanjines, P. E. Schmidd, F. Levy, J. Appl. Phys. 75, 2042-2047, 1994.

[22] S. A. Bilmes, P. Mandelbaum, F. Alvarez, N. M. Victoria, J. Phys. Chem. B 104 (2000) 9851-9858.

[23] W. Göpel, G. Rocker, R. Feierabend, Phys. Rev. 28, 3427, 1983.

[24] M. Formenti, S. J. Teichner, Catalysis (London) 2, 87, 1979.